# Individualized functional topographic mapping with the BayesBrainMap R package and population-derived priors

Nohelia Da Silva Sanchez, Damon D. Pham, Ellyn Butler, Amanda F. Mejia

2025-05-07

## 1. Introduction

The functional organization of the brain is highly individualized, both in terms of the spatial configuration (CITE Gordon 2017 MSC paper) and temporal dynamics (CITE Finn fingerprinting paper) of functional brain networks. The collection and analysis of datasets featuring "highly sampled" individuals (CITE Braga and Buckner 2017, Gordon 2017 MSC paper, Xue et al. 2021) have been crucial in elucidating individual differences in spatial topography in particular, since large amounts of data per individual facilitates accurate estimation of individual functional topographic maps. Furthermore, individual functional topography has been shown to be predictive of various phenotypes as well as disease severity (see citations from OHBM 2023 talk, slide 4). Therefore, individual features of functional topography are a potentially valuable source of imaging-based biomarkers.

Recent research has also revealed that the use of group parcellations or network maps for studies of functional connectivity (FC), i.e. the temporal synchrony between regions of the brain, can lead to systematically biased estimates of FC (CITE Bijsterbosch 2018, 2019). This is because group parcels or networks that are misaligned to the individual's functional topography mix signals from different functional areas. Thus, true differences in functional topography can be misinterpreted as differences in FC. A potential consequence is that real behavioral or phenotypic correlates with functional topography may be incorrectly attributed to FC. To understand the brain mechanisms underlying certain behaviors or disease states, rather than simply predict them, it is crucial to disengangle differences in spatial topography from temporal engagement and connectivity.

An effective approach for extracting individual functional topography from functional magnetic resonance imaging (fMRI) data is the use of hierarchical Bayesian models. These models reduce noise by combining information from multiple subjects, while respecting individual differences and ensuring correspondence between individuals. Hierarchical models been successfully applied in the context of parcellation (CITE Kong et al 2021), probabilistic functional modes (PROFUMO) (CITE Harrison et al., 2015, Farahibozorg et al. 2021), and independent component analysis (ICA) (CITE Guo and Tang, 2013; Mejia et al., 2020). Importantly, they have been shown to perform well based on a modest amount of data per individual, potentially avoiding the need to collect prolonged or repeated sessions of data in individuals (CITE Kong 2021, Mejia 2020). This makes them highly pragmatic, since extensive subject-level scanning is not feasible in many contexts, especially in clinical settings where it can present a financial and physical burden for patients.

Meanwhile, there is growing evidence for the existence and relevance of overlapping functional architecture (Cite Faskowitz 2020 Nature Neuroscience). This favors "soft" parcellations allowing for overlap between functional networks over traditional "hard" parcellations (CITE Bijsterbosch 2023, https://www.sciencedirect.com/science/article/pii/S1053811920306121, https://doi.org/10.1016/j.neuroimage.2017.11.003, others). Examples of soft parcellation approaches include spatial ICA (CITE https://doi.org/10.1109/TMI.2003.822821), temporal ICA (CITE https://doi.org/10.1073/pnas.112132910), PROFUMO (CITE Harrison 2015), non-negative matrix factorization (NMF) (CITE), gradients (CITE

https://doi.org/10.1073/pnas.1608282113), and dictionaries of functional modes (DiFuMo) (CITE https://doi.org/10.1016/j.neuroimage.2020.117126). Spatial ICA, while one of the most popular methods, has the disadvantage of discouraging statistical dependence between network maps, leading to relatively little overlap between networks. PROFUMO and temporal ICA allow for greater spatial overlap, but have the disadvantage of encouraging or enforcing temporal independence between networks, resulting in low levels of functional connectivity between networks (CITE Pervais 2020). Less constrained methods have the potential advantage of expressing both the temporal and spatial dependence between networks, but in the absence of model constraints they often require externally-derived information to guide estimation.

Here we describe Bayesian brain mapping (BBM), a pragmatic and flexible hierarchical Bayesian technique for producing individualized functional brain topographic maps without constraining the spatial or temporal structure of the networks. BBM begins with a *template*, which can take the form of either a group parcellation or a set of continous network maps. BBM is a generalization of template ICA (Mejia et al. 2020), in which the template is a set of group ICA maps, but BBM allows for other types of network maps or parcellations. In BBM, the template is not used directly in the individual-level model, but rather is used to construct *population-derived priors*, which are in turn used in a Bayesian model fit to an individual subject. The priors are based on a training set of subjects from a representative population, either using holdout data from the focal study or data from a publicly available neuroimaging repository such as the Human Connectome Project (HCP) (Van Essen et al. 2013) or Alzheimer's Disease Neuroimaging Initiative (ADNI) (Mueller et al. 2005). The BBM model includes parameters representing subject-specific spatial topography of different networks and their corresponding temporal activation profiles. The model is hierarchical in the sense that it includes population-derived priors on those parameters, but it is fit to data from a single subject to estimate the subject-specific spatial topography and temporal activation. While hierarchical models typically require multi-subject data to establish the shared prior parameters, BBM avoids this requirement by using priors that are already established. This allows BBM to be highly pragmatic, computationally efficient, and potentially clinically applicable.

The use of population-derived priors in BBM reduces noise while retaining relevant signal. This results in more reliable individual-level network topography maps and the functional connectivity between them (Mejia et al. 2020, 2022, 2023). An important feature of the BBM priors on spatial topography is that they spatially vary within each network, generally showing higher inter-individual variance where engagement tends to exist, and lower variance in background regions. This allows individual differences to be expressed where they exist, while reducing noise in background regions. Furthermore, due to the continuous, whole-brain nature of BBM network maps, noise reduction in background regions of one network indirectly contributes to estimation of signal in the same area of the brain in another network. The powerful noise-reduction properties of BBM allows it to produce reliable maps of individual functional topography with moderate scan duration, without necessarily requiring "dense sampling' ' of individuals (CITE Mejia et al 2020).

We have several goals in this work. First, to describe Bayesian brain mapping and illustrate its use, including how to produce population-derived priors and how to perform model fitting using the `BayesBrainMap` R package. Second, to establish and share high-quality population-derived priors using data from the HCP, based on a variety of templates (parcellations and group ICA maps at different resolutions). These priors can be directly adopted to perform BBM in studies of healthy young adults; additionally, we provide and describe the code used to produce them so that population-derived priors can be easily produced for different populations or using different templates. We also provide guidance for visual investigation of the priors to ensure quality. Third, using data from the Midnight Scan Club (Gordon et al. 2017), we illustrate several key strengths of BBM: 1. Its ability to reveal features of individual functional topography, previously revealed through extensive subject-level scanning, from a single session of data 2. The reliability of individualized network maps with limited scan duration 3. The applicability of externally-derived priors to smaller studies or individuals from a similar population, even when acquisition protocols differ from the focal study 4. The overlapping nature of brain networks, even when using templates that enforce (e.g. parcellations) or encourage (e.g. ICA) independence between networks, without compromising the functional connectivity between networks 5. The pragmatic nature of BBM, which can be quickly fit to individual sessions of data once the prior has been established.

## 2. Methods

There are two steps to performing BBM, which are implemented in the `BayesBrainMap` R package: *(1) prior estimation* and *(2) model fitting* (Figure 1).

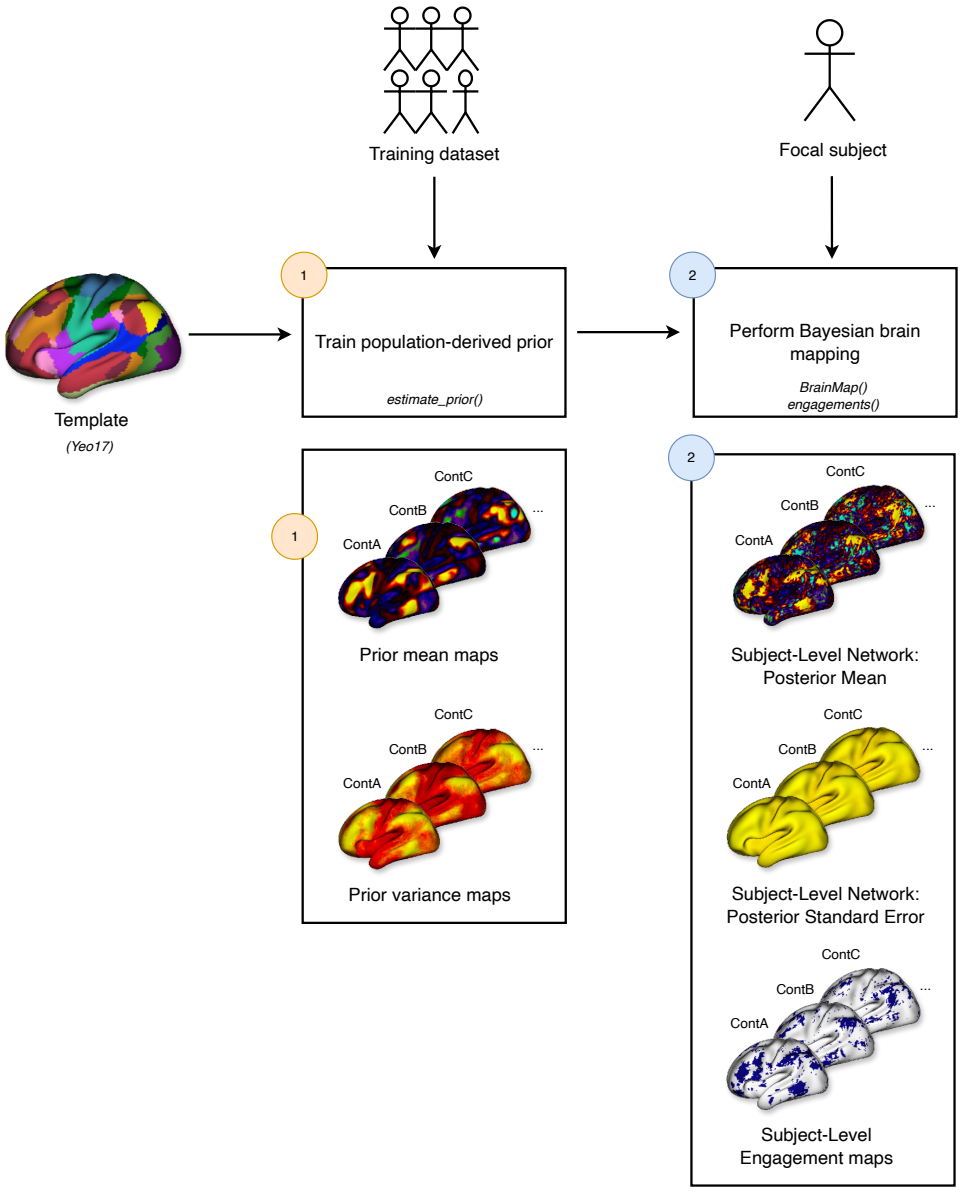


Figure 1: Overview of Bayesian Brain Mapping.

Here, we first present the BBM model. We then explain how we derive population-derived priors using data from the HCP and how they can be accessed and applied, and illustrate the application of BBM to reveal individual-level topography and connectivity. Next, we describe our analysis of data from the Midnight Scan Club using HCP-derived priors, which will illustrate several important features of BBM.

### 2.1 The Bayesian Brain Mapping Model

Here we provide a brief overview of the BBM statistical model. For a given subject and fMRI session, let $y_{tv}$ be the preprocessed BOLD fMRI time series at voxel or vertex $v$ and time point $t$. The BBM model assumes that the BOLD time series can be decomposed into contributions from a set of networks, similar to ICA. The first level of the model is given by

$$y_{tv} = \sum_{q=1}^{Q} a_{tq} s_{qv} + e_{tv} = \mathbf{a}_t^\top \mathbf{s}_v + e_{tv}, \quad e_{tv} \sim N(0, \tau_v^2),$$

where $s_{qv}$ is the spatial engagement of network $q$ at voxel or vertex $v$, and $a_{tq}$ is the temporal activation of network $q$ at time point $t$. The vectors $\mathbf{a}_t$ and $\mathbf{s}_v$ combine those values across all $Q$ networks. The second level of the model incorporates the population-derived prior on the spatial topography in $s_{qv}$, as described in (Mejia et al. 2020):

$$s_{qv} = s_{qv}^0 + \delta_{qv}, \quad \delta_{qv} \sim N(0, \sigma_{qv}^2),$$

where $s_{qv}^0$ and $\sigma_{qv}^2$ are known via the prior, and the deviation terms $\delta_{qv}$ represent individual differences between the subject and the population average. Optionally, spatial dependencies in $\delta_{qv}$ can be modeled via a spatial prior for additional accuracy and power, though at a higher computational cost (Mejia et al. 2022). Note that structured noise may exist in the data that is not well-captured by the residual noise term. While in ICA it is common to model structured noise as components, in BBM these are not included in the model because can be removed beforehand as described in (Mejia et al. 2020) or via pre-processing methods like ICA-FIX.

The third level of the model incorporates the population-derived prior on the functional connectivity between networks, which is represented by the covariance of $\mathbf{a}_t$. This is accomplished by assuming a multivariate Normal prior on $\mathbf{a}_t$ with mean zero and covariance $\mathbf{G}$, and assuming a population-derived hyperprior on $\mathbf{G}$:

$$\mathbf{a}_t \sim N(\mathbf{0}, \mathbf{G}), \text{ where } \mathbf{G} \sim p(\mathbf{G}),$$

See (Mejia et al. 2023) for details on the population-derived prior on the functional connectivity. Briefly, two choices exist for this prior: the conjugate Inverse-Wishart distribution, or a novel Cholesky-based prior developed for this model that more accurately encodes patterns of population variance in FC. The former is faster, while the latter provides somewhat better performance at a higher computational cost.

### 2.2 Building HCP-Derived Priors

Here, we describe construction of HCP-derived priors for Bayesian brain mapping using several different choices of template. These include two different parcellations and group ICA maps (Table 1). Specifically, we use the 17-network Yeo parcellation (Yeo et al. 2011), the MSC group parcellation (Gordon et al. 2017), and HCP-derived group ICA maps with 15 to 50 components (Smith et al. 2013). For each template, we build priors with and without global signal regression (GSR), since whether or not to perform GSR is an important choice that remains the subject of debate.

| **GSR** | **Group ICA** | | | **Parcellation** | |
|---|---|---|---|---|---|
| | 15 HCP ICs | 25 HCP ICs | 50 HCP ICs | Yeo 17 | MSC |
| With GSR | ✓ | ✓ | ✓ | ✓ | ✓ |
| Without GSR | ✓ | ✓ | ✓ | ✓ | ✓ |

Table 1: Templates used for construction of population-derived priors.

Since the functional MRI data in the HCP was acquired with two different phase-encoding directions (left-to-right, LR, and right-to-left, RL), we build the HCP-derived priors using both phase encoding directions separately, as well as a combined version. Comparing the LR and RL priors allows us to assess the impact of phase encoding direction on the priors, while the combined version provides a general purpose prior that is not specific to either the LR or RL acquisition.

Before estimating the BBM priors, we first select a high-quality, balanced subject sample to ensure high-quality and representative priors. Starting from the full HCP sample of $N = 1206$ subjects, we apply several filters to obtain the final sample for the priors. First, we exclude subjects with insufficient scan duration after motion scrubbing using a framewise displacement (FD) threshold of 0.5 mm and dropping the first 15 frames. Second, we exclude any related subjects. Finally, we balanced sex within age groups. See Appendix B for details. After all filters, our final sample contains approximately 350 subjects for each encoding condition (LR, RL) and for the combined dataset, which are used to estimate the priors.

### 2.3 Workflow Overview

Setup

To reproduce this workflow, first follow the setup process outlined in Appendix A.

## 3. Choosing Training Subjects

1. **Filter Subjects by Sufficient fMRI Scan Duration**
   See Appendix B.1 and script: `1_fd_time_filtering.R`
2. **Filter Unrelated Subjects**
   See Appendix B.2 and script: `2_unrelated_filtering.R`
3. **Balance sex within age groups**
   See Appendix B.3 and script: `3_balance_age_sex.R`

The resulting subject list (`valid_combined_subjects_balanced.rds`) is used throughout the rest of the analysis.

## 4. Step 1: Estimate Priors using `estimate_prior()`

In this step, we estimate group-level statistical priors using the `estimate_prior()` function from the `BayesBrainMap` package.

## 4.1 Subject List and Scan Selection

The encoding parameter is set to `combined`, `LR`, and `RL` to use the final lists of subjects saved in Step 3.3 (`valid_combined_subjects_balanced.rds`, `valid__LR_subjects_balanced.rds`, and `valid_RL_subjects_balanced.rds`). The `combined` list includes individuals who passed motion filtering in both LR and RL directions for both sessions, were unrelated, and were sex-balanced within age groups. The `LR` and `RL` lists include subjects who met these criteria independently for each direction.

If encoding is `combined`, we include only REST1 sessions from both phase-encoding directions:

- `rfMRI_REST1_LR_Atlas_MSMAll_hp2000_clean.dtseries.nii`
- `rfMRI_REST1_RL_Atlas_MSMAll_hp2000_clean.dtseries.nii`

If encoding is `LR` or `RL`, we use both REST1 and REST2 sessions from the specified direction:

For `LR`:

- `rfMRI_REST1_LR_Atlas_MSMAll_hp2000_clean.dtseries.nii`
- `rfMRI_REST2_LR_Atlas_MSMAll_hp2000_clean.dtseries.nii`

For `RL`:

- `rfMRI_REST1_RL_Atlas_MSMAll_hp2000_clean.dtseries.nii`
- `rfMRI_REST2_RL_Atlas_MSMAll_hp2000_clean.dtseries.nii`

## 4.2 Temporal Preprocessing Parameters

To standardize scan duration and improve data quality, we apply both initial volume dropping and temporal truncation using parameters handled directly by the `estimate_prior()` function from the `BayesBrainMap` package.

Specifically:

- `drop_first = 15` removes the first 15 volumes from each scan to eliminate early signal instability and motion artifacts.
- `scrub` defines volumes to exclude after a target duration. In our case, we truncate data to the first 10 minutes (600 seconds), excluding any volumes beyond that point.

See Appendix C for more details.

## 4.3 Parcellation Choices

We consider two types of group-level parcellations for estimating priors:

- HCP GICA parcellation (`GICA15.dscalar.nii`, etc.), available in the `data_OSF/inputs` folder. These files were downloaded from the HCP website, specifically from the CIFTI Subject-specific ICA Parcellations dataset for 15-, 25-, and 50-dimensionalities.
- Yeo17 parcellation (Yeo et al. 2011). For details on how this parcellation was processed and simplified for use, see Appendix D.

Each of these parcellations was used to estimate priors with and without global signal regression (GSR), resulting in eight total priors saved as .rds files. See (Table 1) for a summary of the parcellations and GSR combinations.

```
# This script estimates and saves functional connectivity priors
# for both spatial topography and connectivity.
# It supports both GICA-based (15/25/50 ICs) and Yeo17 parcellations,
# with or without global signal regression (GSR).
# For priors using the "combined" subject list, it loads REST1-LR and REST1-RL
# scans for each subject,
# drops the first 15 volumes, and truncates each scan to approximately 10 minutes.
# Outputs:
# - Priors `.rds` file saved in `dir_results`

source("5_estimate_prior.R")
```

### 4.4 Example Usage

Running `estimate_prior()` on the full `"combined"` subject list (~350 subjects) takes approximately 27 hours and uses 135 GB of memory.

For an example of how to run `estimate_prior()` and all relevant parameters, see Appendix E.

## 5. Visualization

In this section, we visualize both the parcellation maps and the priors outputs (mean and variance) for each parcellation scheme used in the study: Yeo17, 15 IC, 25 IC, and 50 IC using the `combined` list of subjects.

We also visualize their corresponding functional connectivity (FC) priors.

### 5.1 Generate and Save Parcellation Visualizations

#### 5.1.1 Yeo17 parcellation

**Script:** `8_visualization_Yeo17parcellations.R`

This script creates one PNG image per parcel (17 in total), where only the selected parcel is colored and all others are white. The parcellation used is Yeo17, created in Appendix D.

Images are saved in `data-OSF/outputs/parcellations_plots/Yeo17`.

#### 5.1.2 GICA Parcellations

Script: `9_visualization_GICAparcellations.R`

This script loops over all independent components for each parcellation dimensionality (`nIC = 15, 25, 50`) and generates two images per component:

- A cortical surface map (e.g., `GICA15_IC1.png`)
- A subcortical view (e.g., `GICA15_IC1_sub.png`)

The resulting images are saved in the following folders:

- `data_OSF/outputs/parcellations_plots/GICA15/`
- `data_OSF/outputs/parcellations_plots/GICA25`
- `data_OSF/outputs/parcellations_plots/GICA50`

Each pair of files corresponds to a specific ICA component and captures its spatial map across brain regions.

### 5.2 Visualize Prior Components

Script: `6_visualization_prior.R`

This script loads each estimated prior file from `priors_rds/` and plots both the mean and standard deviation components for all independent components (ICs).

All images are organized into folders by number of ICs, GSR setting, and corresponding list of subjects used, e.g.:

`data_OSF/priors_plots/GICA15/combined/GSR/`

`data_OSF/priors_plots/GICA15/combined/noGSR/`

`data_OSF/priors_plots/GICA25/LR/noGSR/`

`data_OSF/priors_plots/Yeo17/RL/GSR/`
...

### MSC Data

To illustrate the applicability of BBM when using externally-derived priors, we analyze data from the Midnight Scan Club (MSC) (CITE Gordon et al 2017). The MSC studies on a similar population as the HCP, healthy young adults, but the two datasets differ in acquisition methods. Since the population-derived priors used in BBM encode the distribution of signal, not noise, priors derived from one study can be applied to other studies with differing noise properties, as long as the populations are similar. We illustrate this through application of HCP-derived priors to data from the MSC. Application to the MSC will also exemplify the ability of BBM to reveal individual features of functional topography from just a single session of data.

## Results

### 5.3 Visual Summary of Priors

In this section, we present a comparative visual summary of the estimated group-level priors.

For each parcellation type Yeo17, 15 ICs, 25 ICs, and 50 IC, we display:

- First and Last Parcellation Map
- First and Last Component Mean
- First and Last Component Standard Deviation

These summaries are shown in a 2-column grid layout per parcellation to highlight spatial structure and variability.

All images were generated using the scripts:

- `8_visualization_Yeo17parcellations.R`
- `9_visualization_GICAparcellations.R`
- `6_visualization_prior.R`

#### 5.3.1 15 ICs

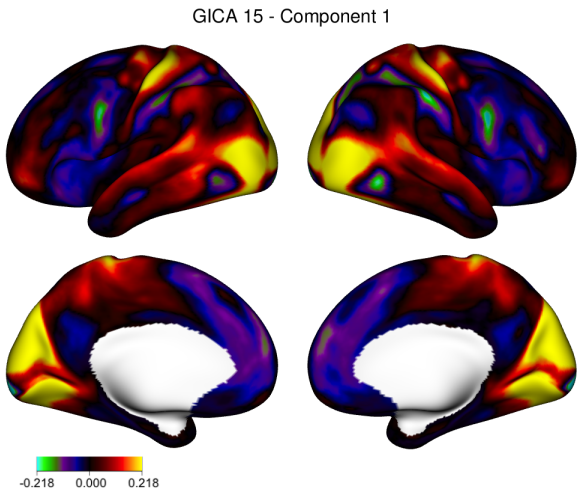
GICA 15 - Component 1
-0.218 0.000 0.218

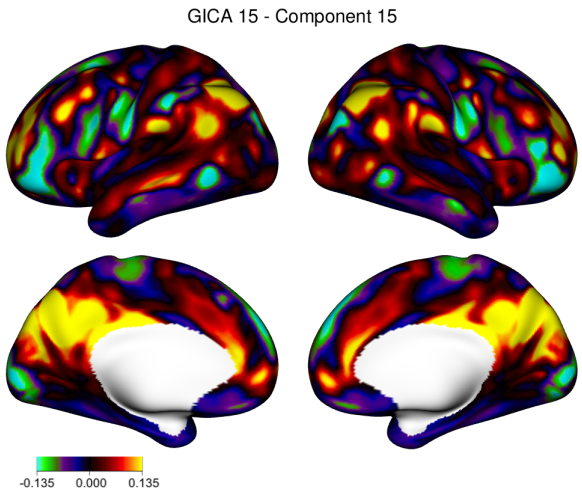
GICA 15 - Component 15
-0.135 0.000 0.135

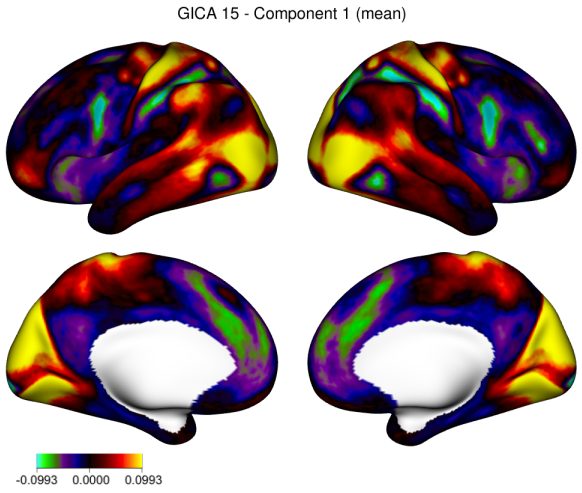
GICA 15 - Component 1 (mean)
-0.0993 0.0000 0.0993

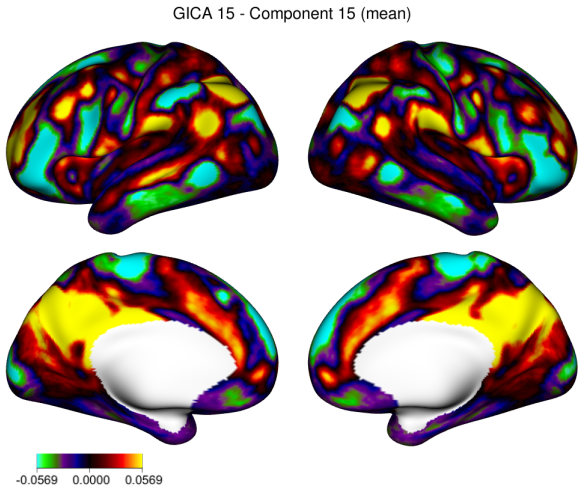
GICA 15 - Component 15 (mean)
-0.0569 0.0000 0.0569

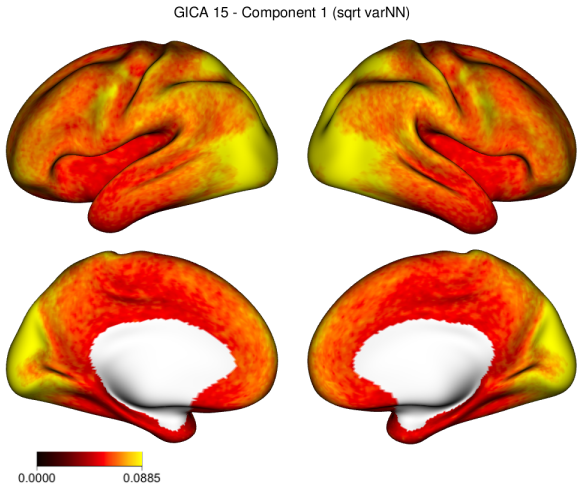
GICA 15 - Component 1 (sqrt varNN)
0.0000 0.0885

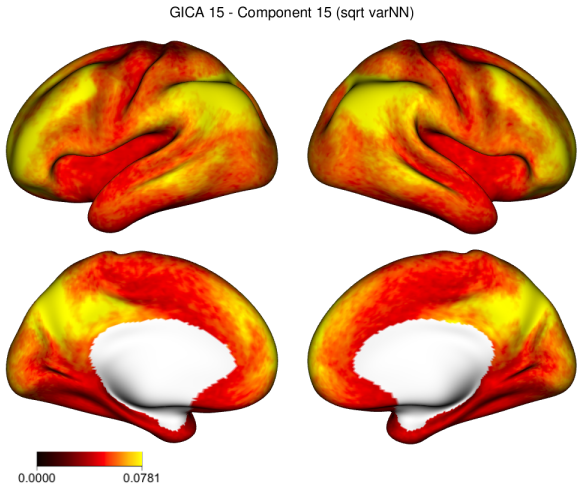
GICA 15 - Component 15 (sqrt varNN)
0.0000 0.0781

### 5.3.2 25 ICs

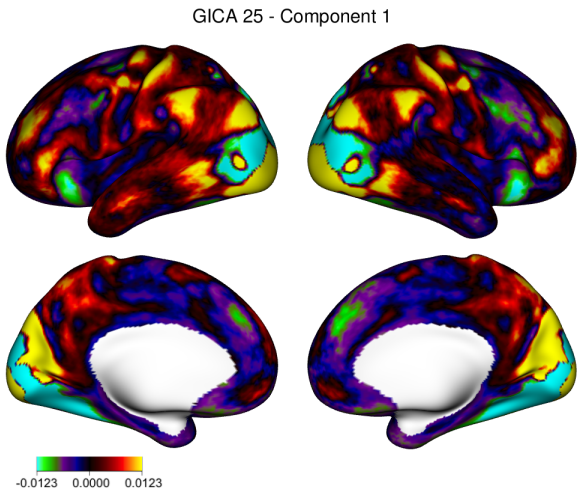
GICA 25 - Component 1
-0.0123 0.0000 0.0123

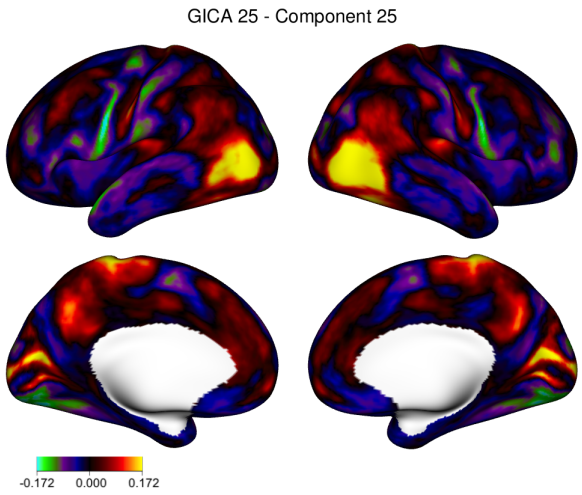
GICA 25 - Component 25
-0.172 0.000 0.172

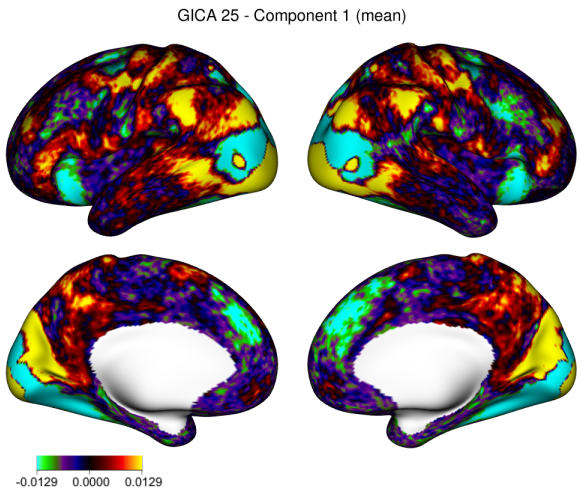
GICA 25 - Component 1 (mean)
-0.0129 0.0000 0.0129

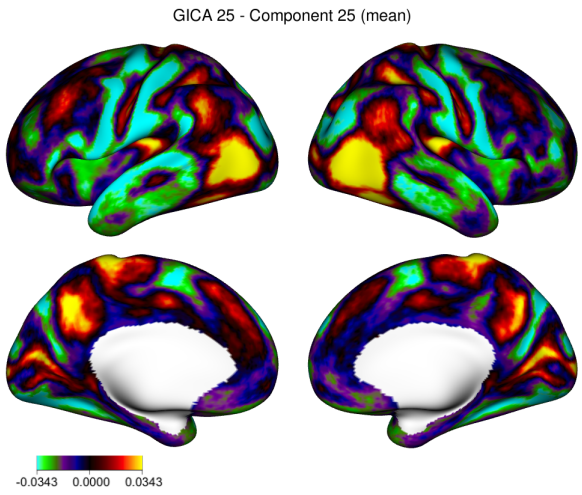
GICA 25 - Component 25 (mean)
-0.0343 0.0000 0.0343

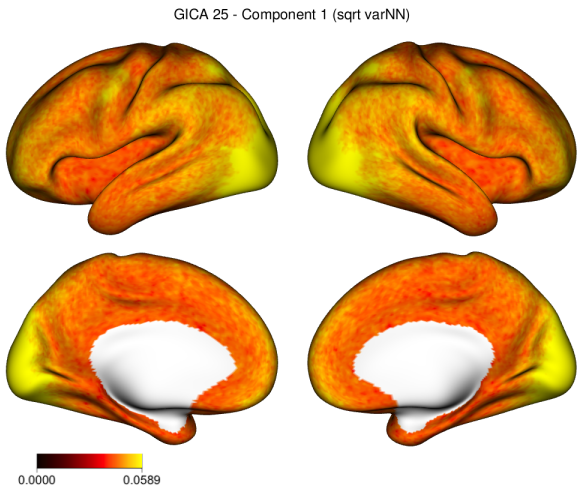
GICA 25 - Component 1 (sqrt varNN)
0.0000 0.0589

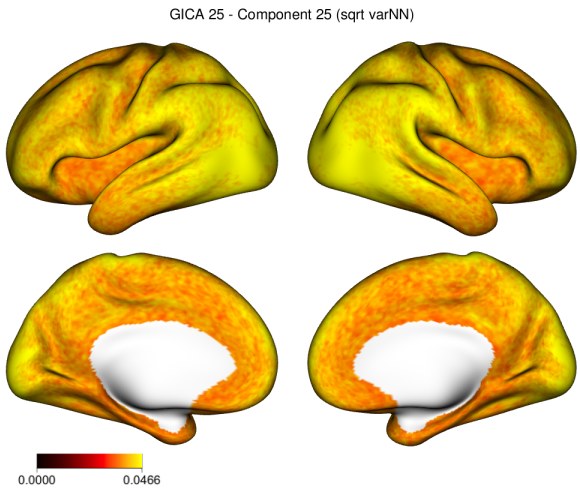
GICA 25 - Component 25 (sqrt varNN)
0.0000 0.0466

### 5.3.3 50 ICs

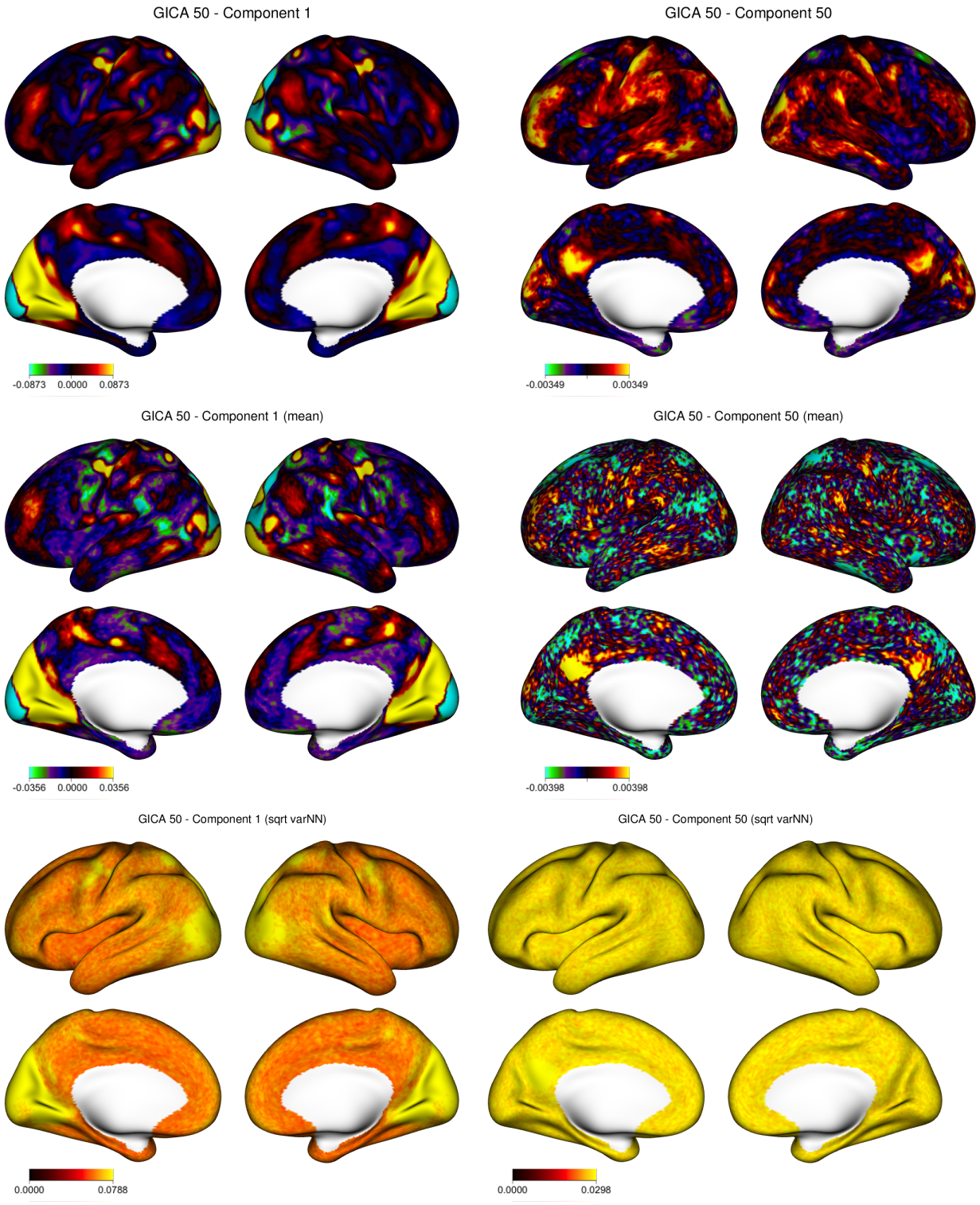


### 5.3.4 Yeo17

For the Yeo17 parcellation, we show visualizations of the two main networks (`DefaultA` and `DorsAttnA`):

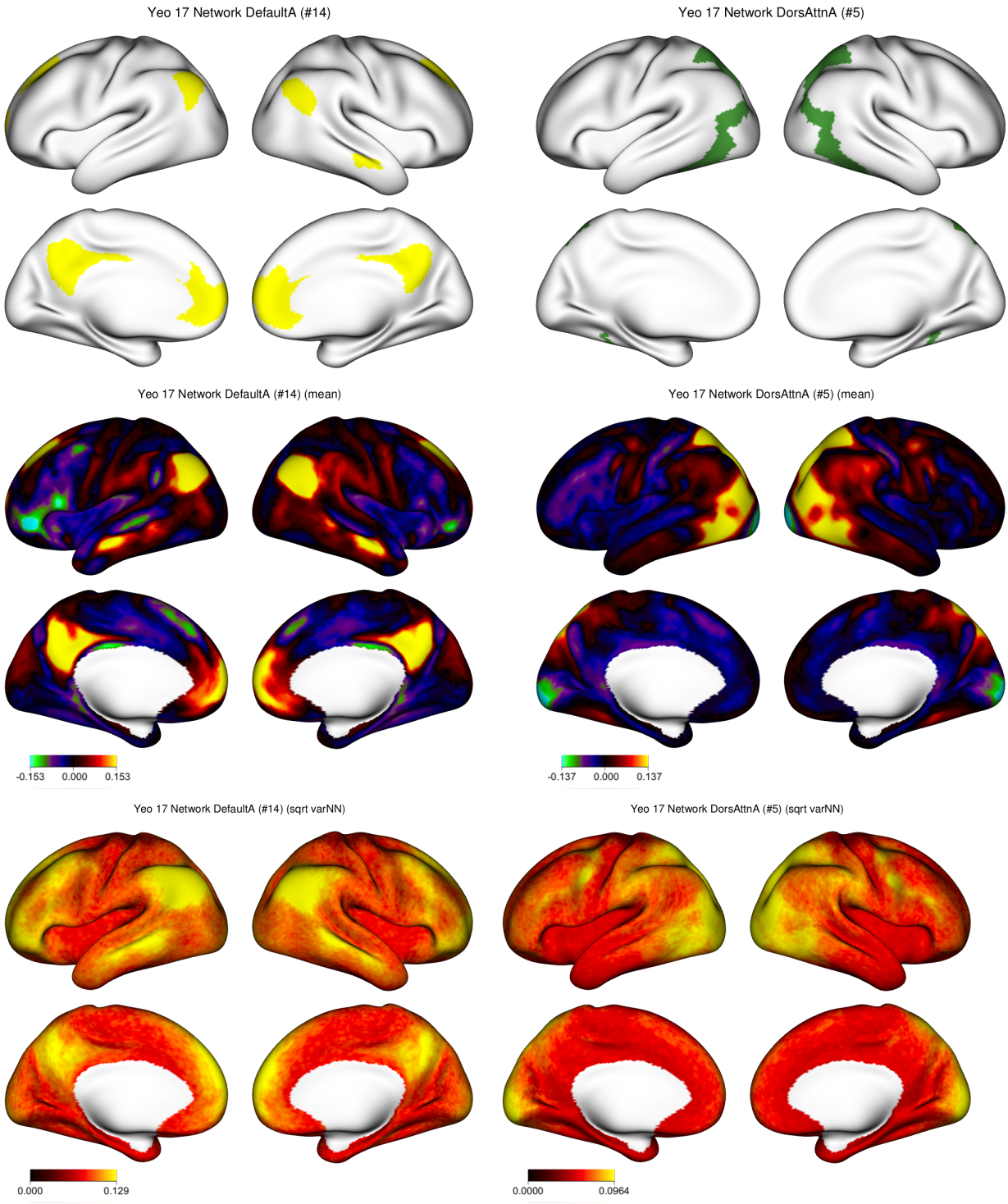


### 5.4 Visualize Functional Connectivity Priors

Script: `7_visualization_FC.R`

This step visualizes the Functional Connectivity (FC) prior for each prior using both the Cholesky and Inverse-Wishart parameterizations. For each group-level prior in `priors/`, we compute and plot:

- Mean FC matrix (off-diagonal values only)
- Standard deviation of FC estimates (from the variance matrix)

For each prior, the following outputs are saved in the corresponding folder under:

`data_OSF/outputs/priors_plots/<parcellation>/<encoding>/FC/`

Where:

- = GICA15, GICA25, GICA50, or Yeo17
- = LR, RL, or combined

**PDF files (2 per prior)**

- `[prior_name]_FC_Cholesky.pdf`
- `[prior_name]_FC_InverseWishart.pdf`

Each PDF includes:

- FC Prior Mean (Page 1)
- FC Prior Standard Deviation (Page 2)

**PNG imgaes (4 per prior)**

- `[prior_name]_FC_Cholesky_mean.png`
- `[prior_name]_FC_Cholesky_sd.png`
- `[prior_name]_FC_InverseWishart_mean.png`
- `[prior_name]_FC_InverseWishart_sd.png`

These visualizations allow for a direct comparison of spatial FC structure and uncertainty across priors and estimation methods.

The figures below show the mean and standard deviation of FC priors for each parcellation (GICA15, GICA25, GICA50, Yeo17) using Cholesky and Inverse-Wishart methods. Only combined priors are shown.

### 5.4.1 GICA15

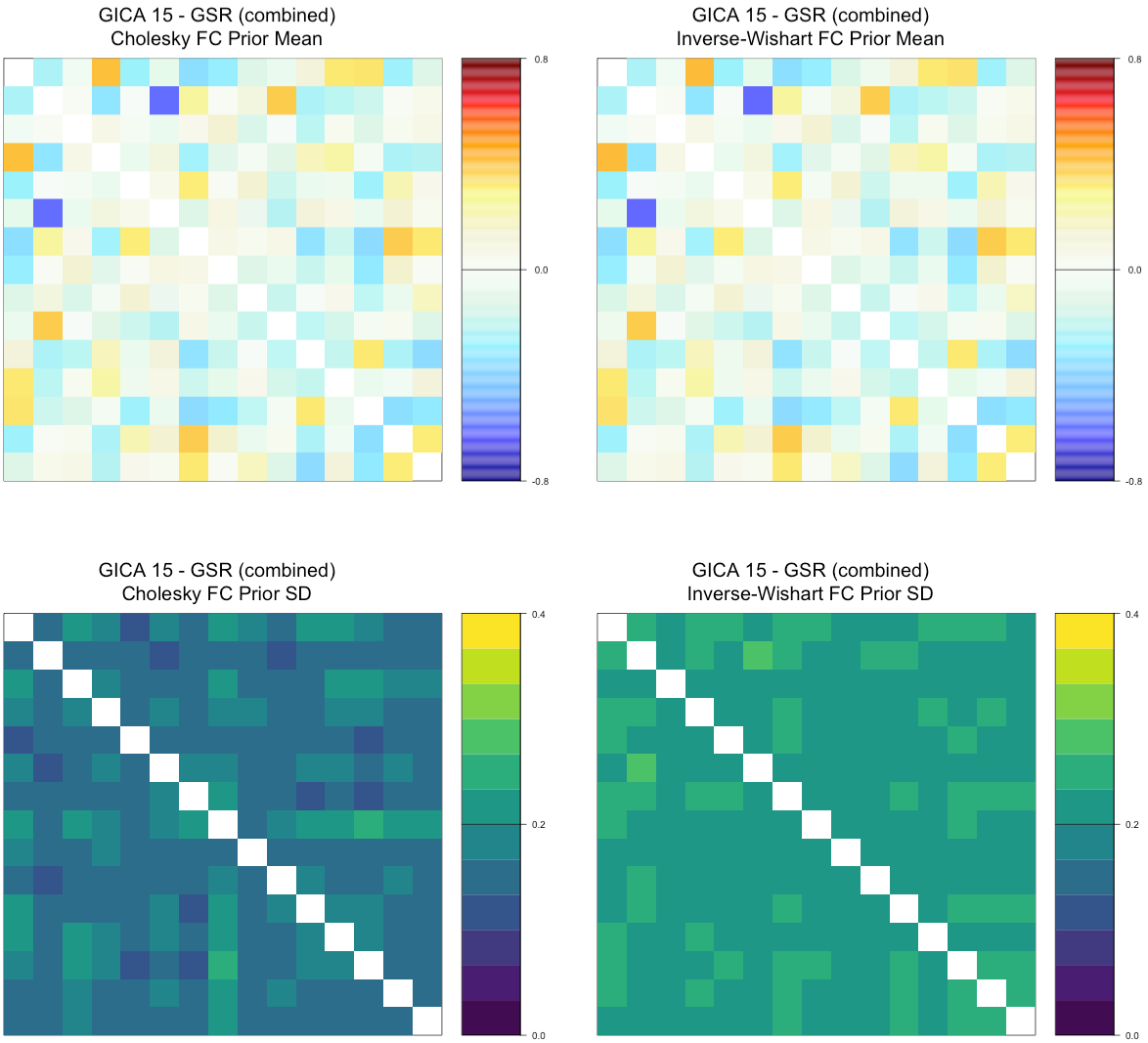
GICA 15 - GSR (combined)
Cholesky FC Prior Mean
0.8
0.0
-0.8
GICA 15 - GSR (combined)
Inverse-Wishart FC Prior Mean
0.8
0.0
-0.8
GICA 15 - GSR (combined)
Cholesky FC Prior SD
0.4
0.2
0.0
GICA 15 - GSR (combined)
Inverse-Wishart FC Prior SD
0.4
0.2
0.0

### 5.4.2 25 ICs

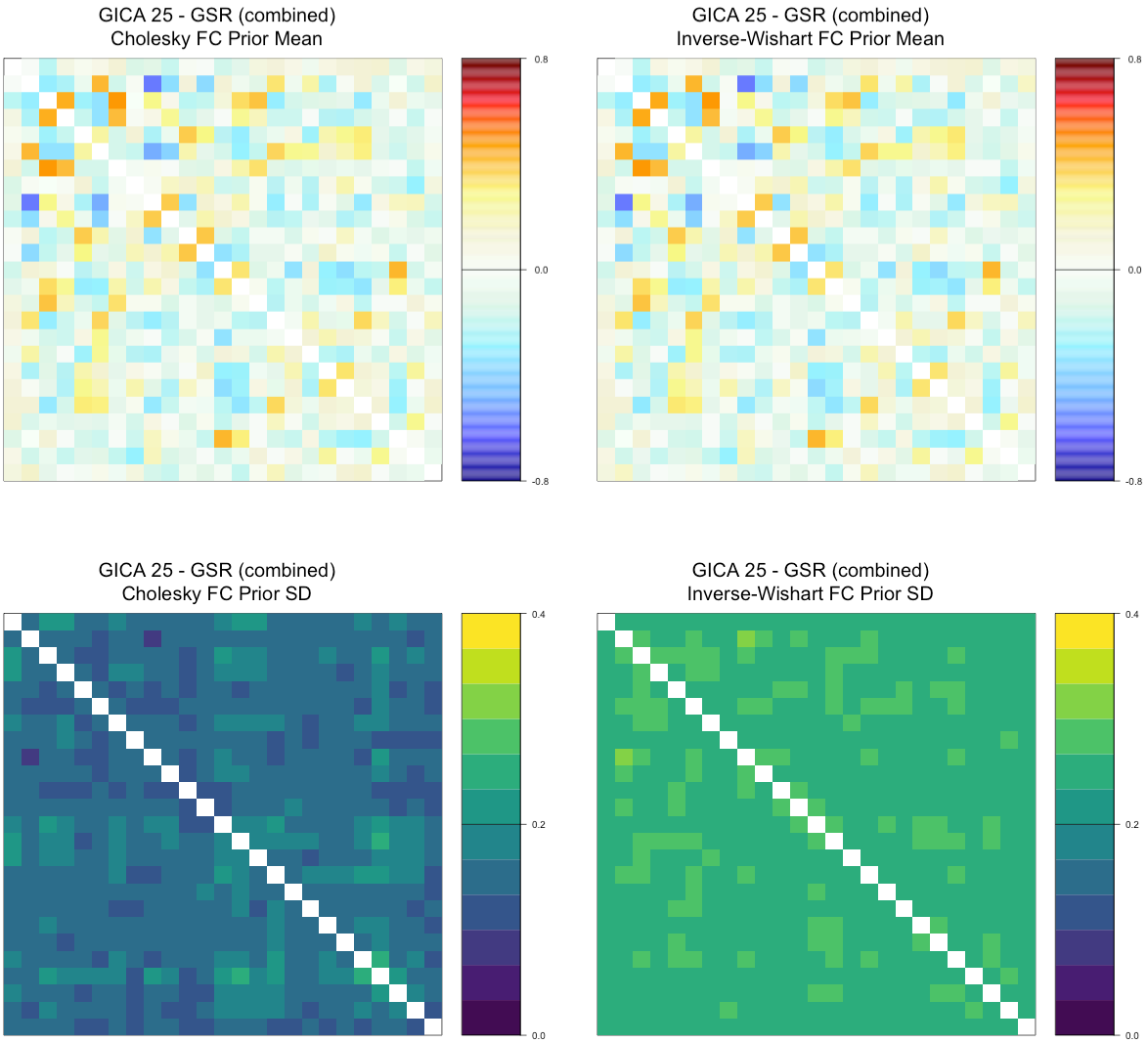
GICA 25 - GSR (combined)
Cholesky FC Prior Mean
0.8
0.0
-0.8
GICA 25 - GSR (combined)
Inverse-Wishart FC Prior Mean
0.8
0.0
-0.8
GICA 25 - GSR (combined)
Cholesky FC Prior SD
0.4
0.2
0.0
GICA 25 - GSR (combined)
Inverse-Wishart FC Prior SD
0.4
0.2
0.0

### 5.4.3 50 ICs

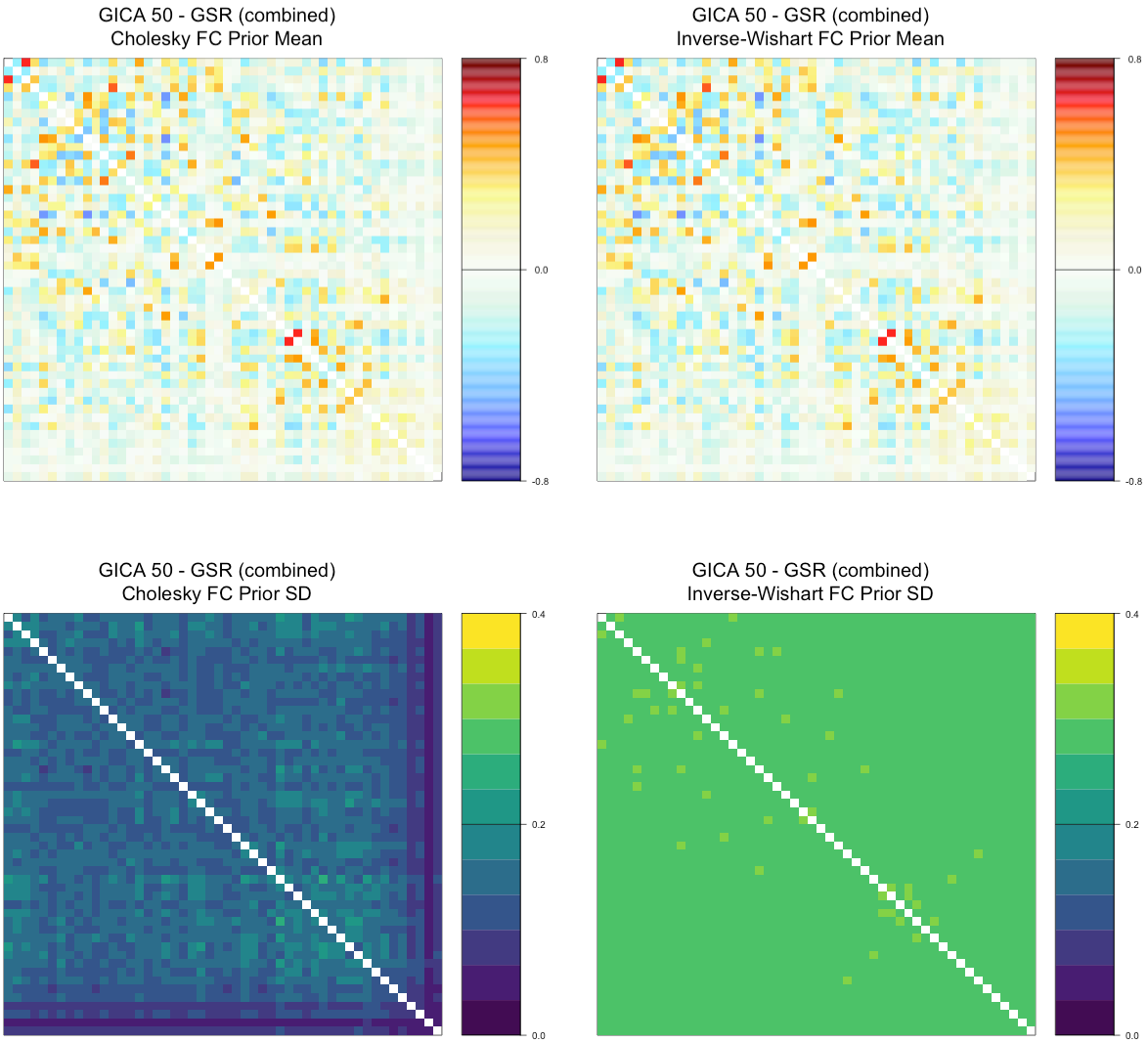
GICA 50 - GSR (combined)
Cholesky FC Prior Mean
0.8
0.0
-0.8
GICA 50 - GSR (combined)
Inverse-Wishart FC Prior Mean
0.8
0.0
-0.8
GICA 50 - GSR (combined)
Cholesky FC Prior SD
0.4
0.2
0.0
GICA 50 - GSR (combined)
Inverse-Wishart FC Prior SD
0.4
0.2
0.0

### 5.4.4 Yeo17

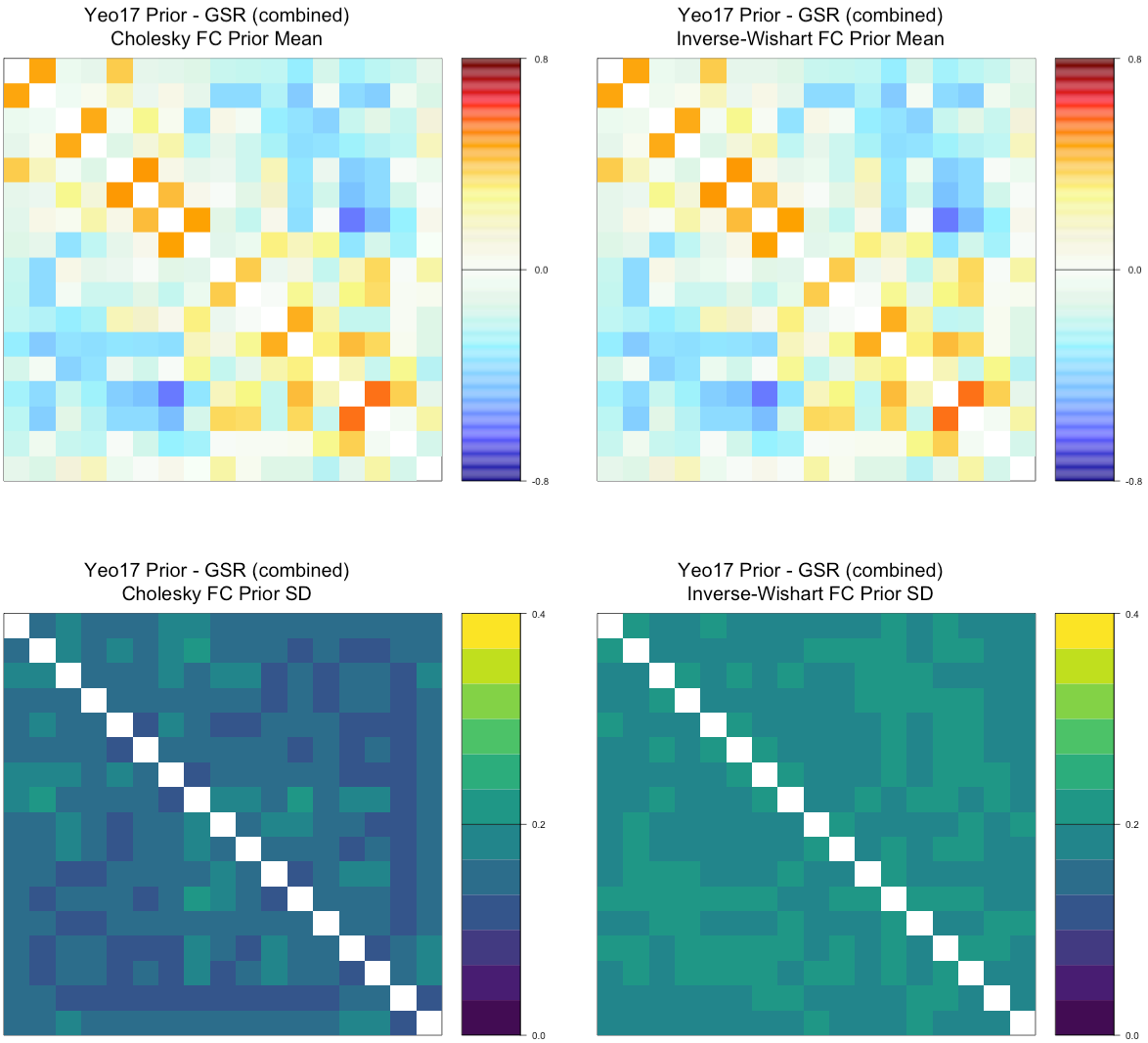


## 6. Step 2: Using Priors for Individual-Level Brain Mapping

In this section, we demonstrate how to apply the population-level priors estimated in Section 4 to perform subject-level analysis using the `BayesBrainMap` package.

The process involves two steps:

1. Fitting the Bayesian brain mapping model to subject data using a precomputed prior.
2. Identifying regions of significant deviation from the prior mean (i.e., areas of engagement).

This example uses:

- A prior based on Yeo17 template with global signal regression (GSR) and the `combined` list of subjects.
- One subject's resting-state data in CIFTI format. In this case, we use HCP subject 100206.

```
# Load population prior
prior <- readRDS("priors/Yeo17/prior_combined_Yeo17_GSR.rds")

# Load subject fMRI data (CIFTI format)
BOLD <- c(file.path(dir_data, "inputs",
                    "rfMRI_REST1_LR_Atlas_MSMAll_hp2000_clean.dtseries.nii"),
          file.path(dir_data, "inputs",
                    "rfMRI_REST1_RL_Atlas_MSMAll_hp2000_clean.dtseries.nii"))
```

**6.1 Load Subject-Level fMRI Data and Prior** The fMRI input must be a CIFTI, NIFTI, or matrix object compatible with the prior.

**6.2 Estimate Subject-Level Networks** Once the data is loaded, we fit the Bayesian brain mapping model to obtain individualized functional networks aligned to the prior components:

```
bMap <- BrainMap(
  BOLD = BOLD,
  prior = prior,
  TR = 0.72,
  drop_first = 15
  )
```

**6.3 Identify Engagement Maps**

```
eng <- engagements(
  bMap = bMap
  )
```

**6.4 Visualize the Results**

We now plot:

1. The subject-level networks estimated by `BrainMap()` (both mean and standard error).
2. The engagement maps, showing regions of deviation from the prior mean.

For all outputs, we only visualize ContA network from the Yeo 17 parcellation.

Yeo 17 Network ContA (#11) Subject-Level Mean

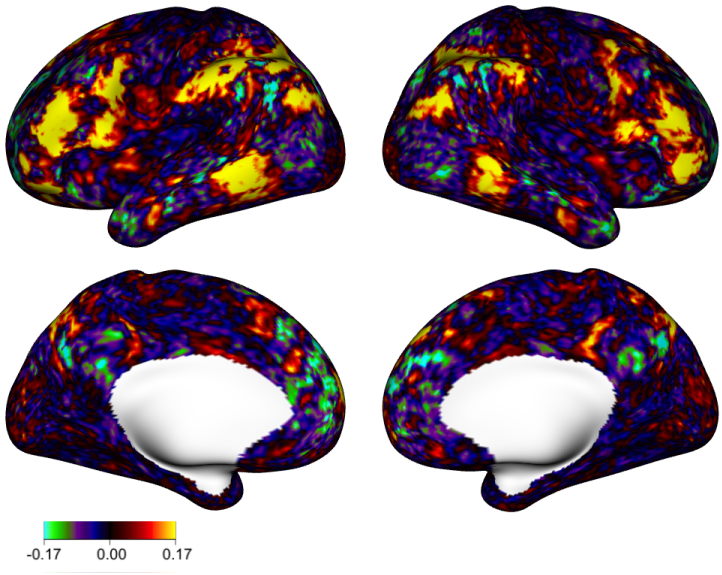


Yeo 17 Network ContA (#11) Subject-Level SE

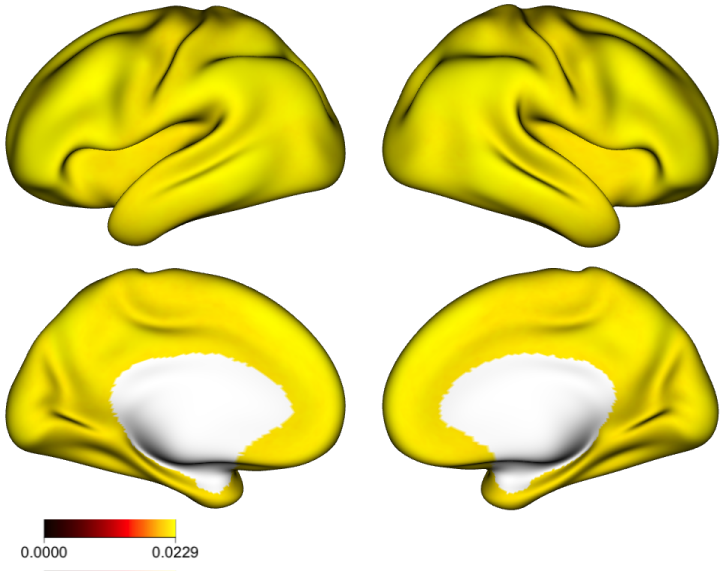

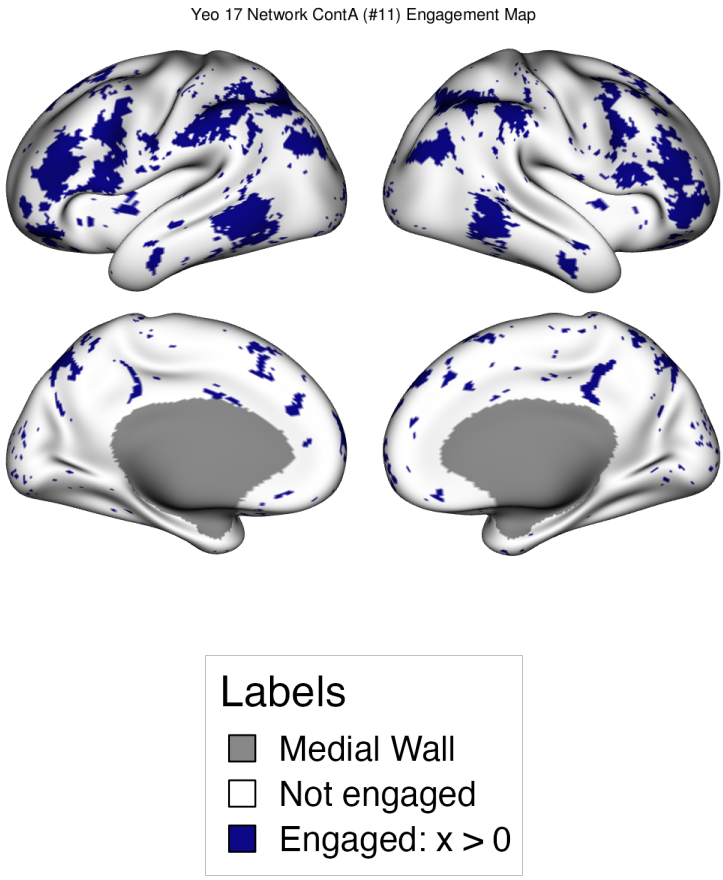


## Appendix A: Setup

To reproduce this workflow, first clone the repository to your local machine or cluster:

```
git clone https://github.com/mandymejia/BayesianBrainMapping-Templates.git
cd BayesianBrainMapping-Templates
```

Next, download the required `data_OSF/` and `priors` folders from the following OSF link:

`https://osf.io/n3wk5/?view_only=0d95b31090a245eb9ef51fe262be60ef`

Once downloaded, unzip the folder and place in the folder in the GitHub directory with the same corresponding name. The folder structure should look like this:

```
BayesianBrainMapping-Templates/
  data_OSF/
      inputs/
      outputs/
  priors/
      GICA15/
      ...
  src/
      0_setup.R
```

```
      1_fd_time_filtering.R
      ...
  BayesianBrainMapping-Templates.Rmd
  ...
```

This section initializes the environment by loading required packages, setting analysis parameters, and defining directory paths.

**Important:** Before running the workflow, you must review `0_setup.R` and install any necessary packages, ensure you have an installation of Connectome Workbench, and update the following variables to match your local or cluster environment:

- `dir_project` (path to the GitHub folder)
- `dir_HCP` (path to the HCP data)
- `HCP_unrestricted_fname` (path to the unrestricted HCP CSV if you have access to it)
- `HCP_restricted_fname` (path to the restricted HCP CSV if you have access to it)
- `wb_path` (location of the CIFTI Workbench on your system)

```
github_repo_dir <- getwd()
src_dir <- file.path(github_repo_dir, "src")
source(file.path(src_dir, "0_setup.R"))
```

## Appendix B: Subject Filtering

### Appendix B.1: Filter Subjects by Sufficient fMRI Scan Duration

We begin by filtering subjects based on the fMRI scan duration after motion scrubbing For each subject, and for each session (`REST1`, `REST2`) and encoding direction (`LR`, `RL`), we compute framewise displacement (FD) using the `fMRIscrub` package. We use a lagged and filtered version of FD (Phạm et al. 2023; Power et al. 2012; Fair et al. 2009) appropriate for multiband data. FD is calculated from the `Movement_Regressors.txt` file available in the HCP data for each subject, encoding and session.

A volume is considered valid if it passes an FD threshold, and a subject is retained only if both sessions in both encodings have at least 10 minutes (600 seconds) of valid data.

The final subject lists include those who passed the filtering criteria separately for each encoding: `LR`, `RL`, and their intersection, referred to as the`combined` list. The combined list includes only subjects who passed all criteria for both LR and RL encodings across both visits (REST1 and REST2), and is the one used throughout this project.

```
# This script filters subjects based on motion using framewise displacement (FD)
# from fMRIscrub.
# For each subject, encoding (LR/RL), and session (REST1/REST2), it computes FD,
# flags volumes exceeding the FD threshold of 0.5 mm (scrubbing),
# and calculates valid scan time after excluding those high-motion volumes.
# Subjects with  10 minutes of valid data in both sessions are retained.
# Outputs (saved in dir_results):
# - Valid subject lists for LR, RL, and combined encodings (intersection)
# - FD summary per subject/session/encoding
```

```r
#set up path, etc.
github_repo_dir <- getwd()
src_dir <- file.path(github_repo_dir, "src")
source(file.path(src_dir, "0_setup.R"))

#run script to exclude sessions based on head motion
source(file.path(src_dir,"1_fd_time_filtering.R"))
```

During this step, an FD summary table is generated with the following columns:

- subject: HCP subject ID
- session: REST1 or REST2
- encoding: LR or RL
- mean_fd: mean framewise displacement
- valid_time_sec: total duration of valid data in seconds

**Preview of FD Summary Table**

| X | subject | session | encoding | mean_fd | valid_time_sec |
|---|---|---|---|---|---|
| 1 | 100206 | REST1 | LR | 0.1017240 | 858.24 |
| 2 | 100206 | REST2 | LR | 0.1361220 | 858.96 |
| 3 | 100206 | REST1 | RL | 0.0698779 | 864.00 |
| 4 | 100206 | REST2 | RL | 0.0824894 | 863.28 |

Table 2: First rows of FD summary table

As shown above, subject 100206 qualifies for further analysis because each of the four sessions (REST1/REST2 $\times$ LR/RL) contains at least 600 seconds of valid data.
The script is currently designed to filter based on valid time only, but it can be easily adapted to apply additional constraints such as maximum mean FD thresholds if desired (e.g., mean_fd $< 0.1$).

### Appendix B.2: Filter Unrelated Subjects

Building on the previous step, we use the HCP restricted demographic data to exclude related individuals. This step helps ensure the statistical independence of subjects in the group-level priors estimation.
For the `LR`, `RL`, and `combined` lists of valid subjects derived in the previous step, we:

1. Subset the HCP restricted demographics to include only those subjects with at least 10 minutes remaining after scrubbing.
2. Filter by `Family_ID` to retain a single individual per family.

Note: This step requires access to the HCP restricted data. If you do not have access, you can skip this step, resulting in some related subjects being included in your training data.

```r
# This script filters subjects to retain only unrelated individuals, using Family ID
# information from the restricted HCP data.
# For each encoding (LR, RL, combined), it selects one subject per family from the
# FD-valid lists.
# Outputs (saved in dir_personal due to restricted data):
```

```
# - Unrelated subject lists for LR, RL, and combined encodings (intersection)

source(file.path(src_dir,"2_unrelated_filtering.R"))
```

### Appendix B.3: Balance Sex Within Age Groups

In the final step of subject selection, we balance sex across age groups to reduce potential demographic bias in priors estimation.
For the `LR`, `RL`, and `combined` lists of valid subjects derived in the previous step, we:

- Subset the HCP unrestricted demographics to include only those subjects.
- Split subjects by age group and examine the sex distribution within each group.
- If both sexes are present but imbalanced, we randomly remove subjects from the overrepresented group to achieve balance.

Note: If the unrelated subject filtering step is skipped (e.g., due to lack of restricted data access), the code automatically falls back to using `valid_<encoding>_subjects_FD` instead of `valid_<encoding>_subjects_unrelated`.
The final list of valid subjects is saved in `dir_results` as:

- `valid_<encoding>_subjects_balanced.csv`
- `valid_<encoding>_subjects_balanced.rds` (used in the prior estimation step)

```
# This script balances sex within each age group for subjects who passed FD and
# unrelated filtering.
# For each encoding (LR, RL, combined), it samples subjects to equalize the number
# of males and females per age group,
# unless an age group includes only one gender (in which case no balancing is applied).
# Uses age and gender information from the unrestricted HCP data.
# Outputs (saved in dir_personal):
# - Sex-balanced subject lists for LR, RL, and combined encodings (as .csv and .rds)

source(file.path(src_dir,"3_balance_age_sex.R"))
```

## Appendix C: Scrubbing and Temporal Truncation

Given the HCP TR of 0.72 seconds, 10 minutes corresponds to:

```
T_total <- floor(600 / TR_HCP) # ~833 volumes
```

To define the volumes to scrub (i.e., exclude beyond 10 minutes), we compute:

```
T_scrub_start <- T_total + 1
scrub_BOLD1 <- replicate(length(BOLD_paths1), T_scrub_start:nT_HCP, simplify = FALSE)
scrub_BOLD2 <- replicate(length(BOLD_paths2), T_scrub_start:nT_HCP, simplify = FALSE)
scrub <- list(scrub_BOLD1, scrub_BOLD2)
```

Because `drop_first = 15` removes frames before truncation, the final retained time series per scan will be slightly shorter than 10 minutes. Approximately:

```
(833 - 15) * 0.72 = ~589 seconds (~9.8 minutes)
```

## Appendix D: Prepare Yeo17 Parcellation for Prior Estimation

In this step, we load and preprocess a group-level cortical parcellation to be used as the template to estimate the priors in the next step. Specifically, we use the Yeo 17-network parcellation (`Yeo_17`) and perform the following operations:

- Simplify the labels by collapsing hemisphere-specific naming and removing subnetwork identifiers, grouping regions by their main network.
- Create a new `dlabel` object that maps each vertex to its corresponding network.
- Mask out the medial wall to exclude it from analysis.

The resulting parcellation is saved as `Yeo17_simplified_mwall.rds`.

```
# This script simplifies the Yeo 17-network parcellation by collapsing region
# labels and masking out the medial wall.
# It creates a cleaned version of the parcellation suitable for downstream analyses.
# Output:
# - Saved as RDS file in dir_data: "Yeo17_simplified_mwall.rds"

source(file.path(src_dir,"4_parcellations.R"))
```

We can visualize the Yeo17 networks and their corresponding labels:

```
# Load libraries
library(ciftiTools)
library(rgl)
rgl::setupKnitr()

# Load the parcellation
yeo17 <- readRDS(file.path(dir_data, "outputs", "Yeo17_simplified_mwall.rds"))
yeo17 <- add_surf(yeo17)

view_xifti_surface(
  xifti = yeo17,
  widget = TRUE,
  title = "Yeo17 Network Parcellation",
  legend_ncol = 6,
  legend_fname = file.path(dir_data, "outputs", "parcellations_plots",
                           "Yeo17", "Yeo17_legend.png"),
  fname=file.path(dir_data, "outputs", "parcellations_plots", "Yeo17")
)
```

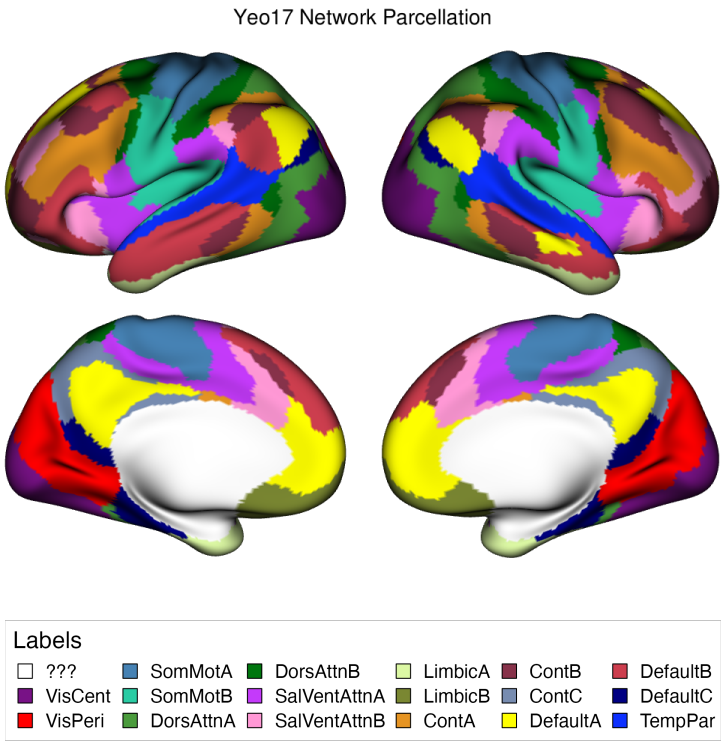


## Appendix E: Example Function Call for Prior Estimation

```
# For detailed parameter descriptions, run: ?estimate_prior

estimate_prior(
  BOLD = BOLD_paths1,          # REST1 LR scans (list of file paths)
  BOLD2 = BOLD_paths2,         # REST2 LR scans (same subjects/order as BOLD)
  template = GICA,             # GICA 15-component parcellation (CIFTI dscalar file path)
  GSR = TRUE,                  # Apply global signal regression
  TR = 0.72,                   # Repetition time in seconds
  hpf = 0.01,                  # High-pass filter cutoff in Hz
  Q2 = 0,                      # No nuisance IC denoising
  drop_first = 15,             # Drop first 15 volumes
  scrub = scrub,               # Timepoints to scrub (list format)
  verbose = TRUE               # Print progress updates
)
```

## References


Fair, Damien A, Alexander L Cohen, Jonathan D Power, Nico UF Dosenbach, Jessica A Church, Francis M Miezin, Bradley L Schlaggar, and Steven E Petersen. 2009. "Functional Brain Networks Develop from a 'Local to Distributed' Organization." *PLoS Computational Biology* 5 (5): e1000381.

Gordon, Evan M, Timothy O Laumann, Adrian W Gilmore, Dillan J Newbold, Deanna J Greene, Jeffrey J Berg, Mario Ortega, et al. 2017. "Precision Functional Mapping of Individual Human Brains." *Neuron* 95 (4): 791–807.

Mejia, Amanda F, David Bolin, Daniel Spencer, and Ani Eloyan. 2023. "Leveraging Population Information in Brain Connectivity via Bayesian ICA with a Novel Informative Prior for Correlation Matrices." *arXiv Preprint arXiv:2311.03791*.

Mejia, Amanda F, Vincent Koppelmans, Laura Jelsone-Swain, Sanjay Kalra, and Robert C Welsh. 2022. "Longitudinal Surface-Based Spatial Bayesian GLM Reveals Complex Trajectories of Motor Neurodegeneration in ALS." *NeuroImage* 255: 119180.

Mejia, Amanda F, Yu Yue, David Bolin, Finn Lindgren, and Martin A Lindquist. 2020. "A Bayesian General Linear Modeling Approach to Cortical Surface fMRI Data Analysis." *Journal of the American Statistical Association* 115 (530): 501–20.

Mueller, Susanne G, Michael W Weiner, Leon J Thal, Ronald C Petersen, Clifford Jack, William Jagust, John Q Trojanowski, Arthur W Toga, and Laurel Beckett. 2005. "The Alzheimer's Disease Neuroimaging Initiative." *Neuroimaging Clinics* 15 (4): 869–77.

Phạm, Damon, Daniel J McDonald, Lei Ding, Mary Beth Nebel, and Amanda F Mejia. 2023. "Less Is More: Balancing Noise Reduction and Data Retention in fMRI with Data-Driven Scrubbing." *NeuroImage* 270: 119972.

Power, Jonathan D, Kelly A Barnes, Abraham Z Snyder, Bradley L Schlaggar, and Steven E Petersen. 2012. "Spurious but Systematic Correlations in Functional Connectivity MRI Networks Arise from Subject Motion." *Neuroimage* 59 (3): 2142–54.

Smith, Stephen M, Diego Vidaurre, Christian F Beckmann, Matthew F Glasser, Mark Jenkinson, Karla L Miller, Thomas E Nichols, et al. 2013. "Functional Connectomics from Resting-State fMRI." *Trends in Cognitive Sciences* 17 (12): 666–82.

Van Essen, David C, Stephen M Smith, Deanna M Barch, Timothy EJ Behrens, Essa Yacoub, Kamil Ugurbil, Wu-Minn HCP Consortium, et al. 2013. "The WU-Minn Human Connectome Project: An Overview." *Neuroimage* 80: 62–79.

Yeo, BT Thomas, Fenna M Krienen, Jorge Sepulcre, Mert R Sabuncu, Danial Lashkari, Marisa Hollinshead, Joshua L Roffman, et al. 2011. "The Organization of the Human Cerebral Cortex Estimated by Intrinsic Functional Connectivity." *Journal of Neurophysiology*.